Atmospheric Environment 62 (2012) 502–511

Contents lists available at SciVerse ScienceDirect

Atmospheric Environment

journal homepage: www.elsevier.com/locate/atmosenv

Aqueous phase sulfate production in clouds in eastern China

Xinhua Shen [a], Taehyoung Lee [a], Jia Guo [b,d], Xinfeng Wang [b,c], Penghui Li [d], Pengju Xu [c], Yan Wang [d], Yu Ren [b], Wenxing Wang [c], Tao Wang [b,c], Yi Li [a], Simon A. Carn [e], Jeffrey L. Collett Jr. [a,*]

[a] Department of Atmospheric Science, Colorado State University, Fort Collins, CO 80523, USA
[b] Department of Civil and Structural Engineering, The Hong Kong Polytechnic University, Kowloon, Hong Kong, China
[c] Environment Research Institute, Shandong University, Jinan, Shandong 250100, China
[d] School of Environmental Science and Engineering, Shandong University, Jinan, Shandong 250100, China
[e] Department of Geological and Mining Engineering and Sciences, Michigan Technological University, Houghton, MI 49931, USA

HIGHLIGHTS

- Aqueous phase sulfur chemistry is examined in clouds in east China.
- Spring and summer clouds were sampled and analyzed in 2007 and 2008.
- H_2O_2 was the dominant S(IV) oxidant.
- Ozone and oxygen (catalyzed by trace metals) were important oxidants in high pH clouds.
- Many summer clouds contained residual H_2O_2 suggesting additional capacity for aqueous sulfur oxidation.

ARTICLE INFO

Article history:
Received 16 August 2011
Received in revised form
30 June 2012
Accepted 30 July 2012

Keywords:
Sulfur dioxide
Sulfate
Aqueous phase oxidation
Clouds
Cloud chemistry
Mt. Tai
China

ABSTRACT

Clouds play an important role in the oxidation of sulfur dioxide to sulfate, since aqueous phase sulfur dioxide oxidation is typically much faster than oxidation in the gas phase. Important aqueous phase oxidants include hydrogen peroxide, ozone and oxygen (catalyzed by trace metals). Because quantities of emitted sulfur dioxide in China are so large, however, it is possible that they exceed the capacity of regional clouds for sulfate production, leading to enhanced long-range transport of emitted SO_2 and its oxidation product, sulfate. In order to assess the ability of regional clouds to support aqueous sulfur oxidation, four field campaigns were conducted in 2007 and 2008 at Mt. Tai in eastern China. Single and 2-stage Caltech Active Strand Cloudwater Collectors were used to collect bulk and drop size-resolved cloudwater samples, respectively. Key species that determine aqueous phase sulfur oxidation were analyzed, including cloudwater pH, S(IV), H_2O_2, Fe, and Mn. Gas phase SO_2, O_3, and H_2O_2 were also measured continuously during the campaigns. A wide range of cloud pH values was observed, from 2.6 to 7.6; 60% of cloud samples had a pH between 3 and 5. H_2O_2 was found to be an important sulfur oxidant, especially at cloudwater pH lower than 5. H_2O_2 was the most important oxidant in 68% of the cloud sampling periods. High concentrations of residual H_2O_2 were observed in many periods, especially in summer, implying a substantial capacity for additional sulfur oxidation. O_3 was an important oxidant when cloudwater pH was higher than approximately 5–5.3, and was the most important oxidant in 20% of the studied periods. Aqueous sulfur oxidation by O_2 (catalyzed by Fe and Mn) was found to be the fastest sulfate production pathway in 12% of the cases. Observed chemical heterogeneity among cloud drop populations was found to enhance rates of S(IV) oxidation by ozone and enhance or slow metal-catalyzed S(IV) autooxidation rates in some periods. These effects were found to be only of minor importance for the total S(IV) oxidation rate, however, as H_2O_2 was the dominant S(IV) oxidant during most periods.

1. Introduction

Clouds are important atmospheric processors of aerosol particles and trace gases. This is especially true in the case of sulfur dioxide. Clouds dominate sulfate production because sulfur dioxide

* Corresponding author. Tel.: +1 970 491 8697; fax: +1 970 491 8483.
E-mail address: collett@atmos.colostate.edu (J.L. Collett).

1352-2310/$ – see front matter © 2012 Elsevier Ltd. All rights reserved.
http://dx.doi.org/10.1016/j.atmosenv.2012.07.079

is typically oxidized much more rapidly in the aqueous phase than occurs in the gas phase. While numerous studies have been conducted examining in-cloud sulfate production in the United States and Europe, relatively little experimental work has been completed on this topic in Asia. This is a particular concern in China, a major emitter of sulfur dioxide (2009 emissions totaled 22.1 million tons (China-MEP, 2010)) due to its large installed base of coal-fired power plants.

Both wet and dry deposition of sulfur are major concerns in China. Larssen et al. (2006) report annual sulfur deposition rates at several locations in China ranging from ~2 to 16 g-S m^{-2}, similar to or higher than peak deposition fluxes in Europe three decades ago. Historically, acid precipitation has been most problematic in southern China. Higher precipitation pH values in Beijing and other northern parts of China, however, do not typically reflect an absence of substantial sulfate input; rather, sufficient acid neutralizing capacity is generally present, from alkaline dust particles and gaseous ammonia, to prevent significant acidification (Wai et al., 2005). As SO_2 emissions continue to increase, however, acidic precipitation is spreading more widely across China.

The sulfate that contributes to China's acid rain and deposition problems is also of interest internationally. High fine particle sulfate concentrations are routinely experienced in nations immediately downwind (Kim et al., 2009). Sulfate transport across the Pacific and into the U.S. is also a concern. Park et al. (2004) estimate that concentrations of sulfate transported across the Pacific to the United States slightly exceed the average concentration (0.12 μg m^{-3}) suggested by the U.S. Environmental Protection Agency for estimating natural visibility conditions in the western U.S.

Globally, sulfur dioxide oxidation is thought to occur mostly in clouds (Lelieveld and Heintzenberg, 1992). Depending on environmental conditions, various aqueous phase oxidation pathways can be important. These include oxidation by hydrogen peroxide, oxidation by ozone, and oxidation by oxygen, catalyzed by certain trace metals (Seinfeld and Pandis, 2006). At low to moderate pH (typically pH ~2–5), oxidation is generally expected to favor the H_2O_2 pathway. Fast S(IV) oxidation by H_2O_2 can, of course, be maintained only as long as H_2O_2 is available. If SO_2 concentrations significantly exceed H_2O_2 concentrations, this pathway may be effective in converting only a portion of the SO_2 to sulfate. Aqueous H_2O_2 can come from gas to droplet partitioning or be formed *in situ* by aqueous photochemistry (Anastasio et al., 1994; Faust et al., 1993; Zuo and Deng, 1999). At pH values above 5, oxidation by ozone and trace metal-catalyzed autooxidation often increase in importance. At these higher pH values, S(IV) oxidation may compete with S(IV) complexation by carbonyls, including formaldehyde (Munger et al., 1984, 1986; Olson and Hoffmann, 1989; Rao and Collett, 1995).

In model simulations of atmospheric sulfate production, Barth et al. (2000) point out the dominant role that aqueous phase chemistry plays, especially in the lower troposphere and in mid-latitude regions of the northern hemisphere. They note that, globally, the column burden of sulfate produced by aqueous phase chemistry is greatest over east Asia and point out the important roles that cloud pH, H_2O_2 concentrations, and depletion of H_2O_2 (by reactions in cloud) play in influencing sulfate production. Barth and Church (1999) simulate changes in atmospheric sulfate burdens resulting from a doubling of SO_2 emissions in SE China. Their simulations suggest a nonlinear response for this situation, in part because increased SO_2 emissions overwhelm available H_2O_2 concentrations, making gas phase sulfate production relatively more important. Because sulfate produced in the gas phase is less susceptible to rapid wet deposition than sulfate produced in-cloud, the net effect is that a doubling of SO_2 concentrations produces more than a doubling of SE China's contribution to the global tropospheric sulfate burden.

Because aqueous phase oxidation processes are so critical to sulfate production, it is imperative to understand factors influencing cloud chemistry in China in order to accurately predict effects of increasing regional SO_2 emissions on sulfate production in that part of the world and its local, regional, and intercontinental effects. While model simulations provide valuable insight into sulfur chemistry and its sensitivity to changing emissions, *in situ* observations are needed to assess actual conditions in the region. Here we report some of the first regional observations of this type. Findings from two years of spring and summer cloud chemistry measurements at Mt. Tai, an isolated peak in the North China Plain, are presented. Observations of cloud pH, along with key S(IV) oxidants and catalysts, are reported and used to examine the importance of various aqueous phase sulfate production pathways. The presented findings represent the first thorough analysis of in-cloud S(IV) oxidation chemistry in eastern China based on in-cloud observations of cloud composition and concentrations of key oxidants and catalysts. They also represent the first observations of drop size-resolved cloud drop composition in China and its influence on aqueous sulfate production.

2. Experimental methods

2.1. Sampling site description

Field experiments were conducted in spring and summer of 2007 and 2008 at the summit of Mt. Tai (1534 m a.s.l.), an isolated peak in eastern China (Fig. 1). Mt. Tai is located in central Shandong province at the eastern edge of the North China Plain, between the Bohai Economic Rim and Yangtze River Delta Economic Zone, two of China's three major economic circles. The summit of Mt. Tai contains a number of temples and tourist facilities, but access is only by cable car or foot. No vehicles can access the summit and the height of the mountain minimizes impacts from fresh urban emissions. The summit is frequently in cloud during spring and summer; nearly half of the days per year have fog. Together, these factors make Mt. Tai a suitable site for sampling clouds influenced by regional air pollution in eastern China. Other investigators have also found Mt. Tai a useful site for measurement of various aerosol and gas phase pollutants (Gao et al., 2005; Kanaya et al., 2008; Li et al., 2008; Mao et al., 2009; Ren et al., 2009; Wang et al., 2011, 2009, 2008, 2006b; Yamaji et al., 2010). These previous investigations of atmospheric composition at Mt. Tai focused primarily on study of gas and particle phase constituents and precipitation chemistry, but little was known about cloud chemistry in the region prior to this study. Measurements were made in 2007 on the grounds of a meteorological observatory at the mountain summit. Equipment was relocated in 2008 to the roof of a small hotel located nearby, due to access difficulties at the original sampling site.

2.2. Instruments and analysis

Bulk cloudwater samples were collected in the spring and summer 2007 and 2008 campaigns using a Caltech Active Strand Cloudwater Collector (CASCC) (Demoz et al., 1996). The CASCC collects droplets by inertial impaction on 6 rows of 508 μm Teflon strands, and features a 50% lower size cut of 3.5 μm diameter. The CASCC was operated with a downward facing inlet to exclude precipitation which accompanied some cloud interception events. In the 2008 campaigns, a 2-stage size-fractionating Caltech Active Strand Cloudwater Collector (sf-CASCC) (Demoz et al., 1996; Rattigan et al., 2001; Reilly et al., 2001) was added to the

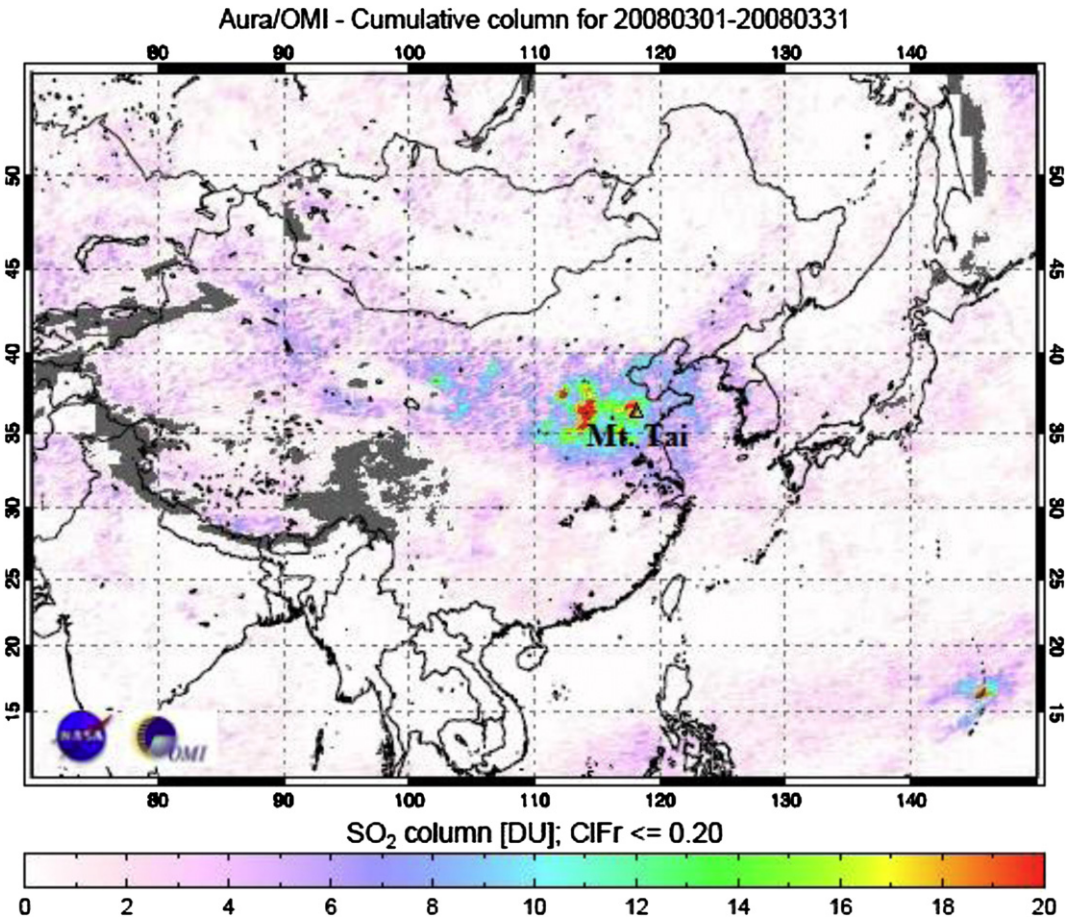

Fig. 1. Location of the Mt. Tai sampling site (triangle). For reference, cumulative SO_2 column amounts are shown for the period between Mar 1st and Mar 31st, 2008. SO_2 data were measured by the Ozone Monitoring Instrument on NASA's EOS/Aura spacecraft and retrieved using a Band Residual Difference (BRD) algorithm (Krotkov et al., 2006) and assuming an SO_2 layer altitude of less than 3 km (PBL) for the sampling location.

experiment to permit observation of the difference in chemical composition between large and small drop size fractions. Large drops (diameters greater than approximately 16 μm) are collected on Teflon cylinders in the first stage of the instrument. Smaller drops (diameters between approximately 4 and 16 μm) are collected on the second stage (six rows of Teflon strand as in the CASCC). The sf-CASCC was also operated with a downward facing inlet to exclude raindrops during periods of precipitation. The CASCC and sf-CASCC have been operated in numerous prior cloud and fog sampling campaigns at other locations (Collett et al., 1999; Hoag et al., 1999; Rao and Collett, 1995, 1998; Rattigan et al., 2001; Reilly et al., 2001). Prior to each cloud event, the cloud collectors were cleaned with deionized water and field blanks were collected.

Cloud liquid water content (LWC) was measured by a Gerber Scientific Particulate Volume Monitor (model PVM-100; (Gerber, 1991)). The PVM was disabled by a lightning strike midway through the summer 2008 campaign. A comparison of cloud collector water collection rates and PVM LWC prior to the lightning strike revealed a good relationship ($r^2 = 0.94$) and allowed LWC to be estimated from cloudwater collection rates for periods when the PVM was unavailable.

Most cloudwater samples were collected during cloud interception events at one to two hour intervals, depending on the LWC. Immediately after collection, samples were weighed to determine collected volume and sample aliquots were measured to determine cloud pH using a portable pH meter and combination electrode calibrated with pH 4 and 7 buffers. Aliquots were next prepared from each sample for later analysis of key species, including major ions (Na^+, NH_4^+, K^+, Mg^{2+}, Ca^{2+}, Cl^-, NO_3^-, and SO_4^{2-}), S(IV), metals (Fe and Mn), HCHO, and H_2O_2. Additional measurements, not reported here, were also made of total organic carbon and organic acids. Unstable compounds were stabilized and analyzed as described below and as reported previously (Collett et al., 1999). Preparation of stabilized sample aliquots was typically completed within 30 min of sample collection. All sample aliquots were refrigerated on-site and later transported cold for laboratory analysis. 2007 samples were kept cold and transported to Shandong University for analysis. 2008 samples were express shipped cold to the United States for analysis at Colorado State University. Duplicate field sample aliquots and replicate laboratory analyses were used to verify measurement precision while several split samples from 2007 analyzed both by Shandong University and Colorado State University indicate good measurement comparability between the two laboratories.

Aliquots for aqueous H_2O_2 analysis were preserved by addition of a buffered solution of *p*-hydroxyphenylacetic acid (POPHA) and horseradish peroxidase to form a dimer (Lazrus et al., 1985) which can be quantified using a fluorescence spectrophotometer. Aliquots for S(IV) analysis were prepared by adding a preservative solution containing formaldehyde, trans-1,2-cylohexylenedinitrilo-tetraacetic acid (CDTA) and sodium hydroxide. The S(IV) in the sample reacts with formaldehyde to form a stable compound, hydroxymethanesulfonate (HMS). Catalase is added to destroy any H_2O_2 in the aliquot. HMS is decomposed in the laboratory to free S(IV) and

formaldehyde. The free S(IV) is reacted with pararosaniline (Dasgupta et al., 1980) to produce a colored product that is measured by absorbance at 580 nm. Aliquots for formaldehyde analysis were prepared by adding a formaldehyde preservation solution containing bisulfite to form HMS. For analysis, HMS is decomposed to release formaldehyde which is analyzed by reaction with 2,4-pentanedione and ammonium acetate to form 3,5-diacetyl-1,4-dihydrolutidine (DDL) which is detected by fluorescence (Dong and Dasgupta, 1987). Fe and Mn were stabilized by acidification with trace metal grade nitric acid and measured by a Varian SpectrAA-640Z Graphite Furnace Atomic Absorption Spectrophotometer (GFAAS) with Zeeman background correction.

The inorganic ions were analyzed by two Dionex cation and anion ion chromatography (IC) systems. Concentrations of major anions (Cl^-, NO_3^-, and SO_4^{2-}) and major cations (Na^+, NH_4^+, K^+, Mg^{2+}, and Ca^{2+}) were determined using standard separations, with suppression and conductivity detection, recommended by the manufacturer. The ICs were calibrated using standard solutions prepared from analytical grade reagent salts. Independent, NIST-traceable check standards were used to verify calibration accuracy.

Gas phase compounds measured in the field campaigns included hydrogen peroxide, ozone, and sulfur dioxide. Gas phase hydrogen peroxide was measured using a custom-built continuous analyzer developed based on a fluorometric method (Lazrus et al., 1986). Details of the measurement method and instrument deployment have been described by Ren et al. (2009), who reported concentrations measured in 2007 at Mt. Tai. Although this measurement technique responds to both hydrogen peroxide and water soluble organic hydroperoxides, the measured signal is typically due mainly to hydrogen peroxide, given its greater atmospheric abundance and higher aqueous solubility. O_3 was measured using a UV photometric O_3 analyzer (Thermo Electron Corporation, Environmental Instruments, model 49C). SO_2 was measured by a pulsed fluorescence SO_2 analyzer (Thermo Electron Corporation, Environmental Instruments, model 43C Trace Level). Additional information about these analyzers has been provided in conjunction with prior deployments (Wang et al., 2002, 2001, 2006a, 2003).

3. Results and discussion

Numerous periods of cloud interception occurred during the four Mt. Tai field campaigns. During the spring 2007 campaign (March 15–April 21), there were 9 cloud events; 38 bulk cloudwater samples were collected. During the summer 2007 campaign (June 15–July 18), there were 12 cloud events; 66 bulk cloudwater samples were collected. During the spring 2008 campaign (March 25–April 25), there were 4 cloud events; 72 cloudwater samples (including 22 bulk samples and 50 size-fractionated samples) were collected. During the summer 2008 campaign (June 10–July 15), there were 18 cloud events; 297 cloudwater samples (including 105 bulk samples and 192 size-fractionated samples) were collected. Observations of cloudwater composition at Mt. Tai in 2007 and 2008 reveal that major solutes include sulfate, nitrate, and ammonium. Sulfate and ammonium were the most abundant ions observed, with volume-weighted mean (VWM) concentrations of 1064 μN and 1216 μN, respectively. The VWM nitrate concentration was 407 μN. Concentrations of total organic carbon (TOC) were also very high in some samples, reaching as much as 200 ppmC. Wang et al. (2011) discuss factors influencing the composition of spring 2007 Mt. Tai cloud samples. A detailed discussion of the major cloudwater solutes and their dependence on transport patterns for all 2007 and 2008 sampling periods is provided by Guo et al. (2012). Detailed information concerning observed cloud composition and a tabulation of the composition of each measured cloudwater sample is available in Shen (2011). Our primary focus here is on determining the availability of key species involved in aqueous phase S(IV) oxidation and examining which oxidation pathways are most important for the environment studied.

3.1. Gaseous species

Key gas phase species associated with aqueous sulfate production include sulfur dioxide, ozone, and hydrogen peroxide. The average concentrations of SO_2 measured during the Mt. Tai spring campaigns were approximately double the summertime averages. Average mixing ratios of 15.4 ppbv and 14.5 ppbv were observed in spring 2007 and spring 2008, respectively, while average mixing ratios of 8.1 ppbv and 6.4 ppbv were observed in summer 2007 and summer 2008. Average O_3 concentrations were similar across all four campaigns, with mixing ratio averages of 62.1 ppbv and 66.0 ppbv in spring 2007 and spring 2008, respectively, and average mixing ratios of 72.1 ppbv and 68.0 ppbv in summer 2007 and summer 2008.

Ren et al. (2009) present a detailed analysis of the H_2O_2 concentrations measured at Mt. Tai in the spring and summer 2007 campaigns. H_2O_2 concentrations were generally lower in spring (2007 average mixing ratio of 0.17 ppbv) than in summer (2007 average 0.55 ppbv). The average summer 2008 H_2O_2 mixing ratio was similar (0.59 ppbv) to summer 2007. A reliable spring 2008 average H_2O_2 concentration could not be determined due to periodic problems with residual H_2O_2 in purified water brought on-site during that campaign. Higher H_2O_2 concentrations are expected in summer, when more active photochemistry occurs, promoting H_2O_2 formation through both gas and aqueous phase reactions. Summertime gaseous H_2O_2 mixing ratios at Mt. Tai were observed to climb as high as 4 ppbv. As discussed by Ren et al. (2009), the Mt. Tai H_2O_2 mixing ratios are similar to those measured at several other mountain locations, but lower than observed at some sites. Ren et al. (2009) analyze factors influencing production and sinks of H_2O_2. Their analysis suggests that photochemical production is an important source of peroxides observed at Mt. Tai with substantial removal in synoptic scale clouds. In summer, chemical suppression of H_2O_2 production by high NO_x concentrations in the boundary layer and wet removal by sulfur-rich clouds combine to limit daytime H_2O_2 concentrations. Subsiding, night-time air masses with low NO_y concentrations often contained higher H_2O_2 concentrations. Relationships between local H_2O_2 and O_3 concentrations were weak at Mt. Tai (Ren et al., 2009). While both are formed as a result of photochemistry involving NO_x and hydrocarbons, they are influenced by different sinks. In this region with high SO_2 concentrations and abundant clouds, loss of H_2O_2 by aqueous reaction with S(IV) can be especially important.

Because of the fast aqueous phase reaction between H_2O_2 and dissolved SO_2, one might expect to observe an anti-correlation between gaseous H_2O_2 concentrations and the presence of clouds. Fig. 2 explores this relationship, plotting timelines of the gaseous H_2O_2 mixing ratio and the cloud LWC measured by the PVM for the first two weeks of the summer 2008 campaign, before the lightning strike disabled the PVM. It is important to keep in mind that the PVM LWC only indicates the presence of clouds intercepting the Mt. Tai summit; it does not indicate whether clouds are present nearby that might also provide a medium for H_2O_2 reaction with dissolved SO_2. Nevertheless, Fig. 2 illustrates a clear relationship between cloud interception and gas phase H_2O_2 mixing ratios. During the first half of the illustrated period, clouds were observed frequently at the summit of Mt. Tai and H_2O_2 mixing ratios generally stayed below 0.5 ppbv. During the second half of the period, cloud interception was much less common and H_2O_2

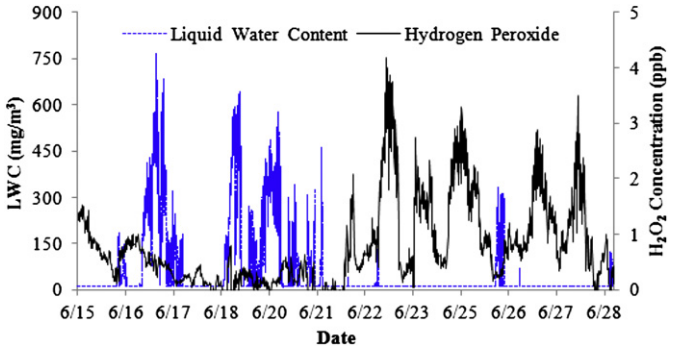

Fig. 2. Timelines of gaseous H_2O_2 mixing ratio and cloud LWC observed at the Mt. Tai summit, 6/15–6/28/2008.

mixing ratios regularly climbed into the 2–4 ppbv range. The disappearance of gas phase H_2O_2 during cloudy periods is consistent with its uptake by cloud droplets and consumption during aqueous phase sulfate production, a topic discussed further below.

3.2. Cloudwater composition

Assuming the aqueous phase concentrations in the cloud drops can be considered at equilibrium with gas phase sources of SO_2, O_3, and H_2O_2, the key cloud composition parameters needed to determine aqueous S(IV) oxidation rates by the pathways introduced earlier are the cloud drop pH and the cloud drop concentrations of trace metal catalysts. Both are reported here, for bulk cloudwater collected with the CASCC and, in 2008, for the drop size-resolved cloud samples from the sf-CASCC. The timescale to establish equilibrium between the gas and aqueous phases for soluble gas phase compounds depends on a variety of parameters, including the solubility of the gas in question, the size of the cloud droplet, and any relevant rates of loss (e.g., by chemical reaction) of the dissolved compound inside the droplet. In the case of the slightly to moderately soluble gases of most interest here (sulfur dioxide, ozone, and hydrogen peroxide) equilibrium is generally considered to be achieved on short timescales relative to droplet lifetime, except in cases where the drop size is very large (typically >30 μm diameter) and rates of chemical consumption inside the droplet are very high. The latter is of concern generally only at high pH (typically pH above 6 or 7) where the rates of reaction of S(IV) with ozone and formaldehyde become very fast (Reilly et al., 2001). Even then, failure to achieve equilibrium for the gases discussed here is primarily of concern for very large cloud drops. PVM and sf-CASCC observations both reveal that most cloud liquid water was not associated with large drops, with typical drop sizes generally between 15 and 25 μm diameter. Given the modest drop sizes and acidic pH values (see below) typically observed in Mt. Tai clouds, an assumption of equilibrium gas–liquid partitioning for sulfur dioxide, ozone, and hydrogen peroxide is realistic.

A very wide range of cloud pH values was observed in bulk cloudwater samples collected at Mt. Tai using the CASCC. Cloudwater pH values ranged from 2.69 to 7.64 in 2007 and from 2.65 to 6.94 in 2008. These ranges are large enough that we should expect multiple S(IV) oxidation pathways to be important at various times. Frequency distributions of observed pH values in the four sampling campaigns are shown in Fig. 3a. The average pH values (determined from the volume-weighted average H^+ concentrations) in spring and summer 2007 were 3.68 and 4.10, respectively. The average pH values in spring and summer 2008 were 4.34 and 3.77, respectively.

Fig. 3b compares the pH values measured in small and large droplet fractions collected with the sf-CASCC during the 2008 field

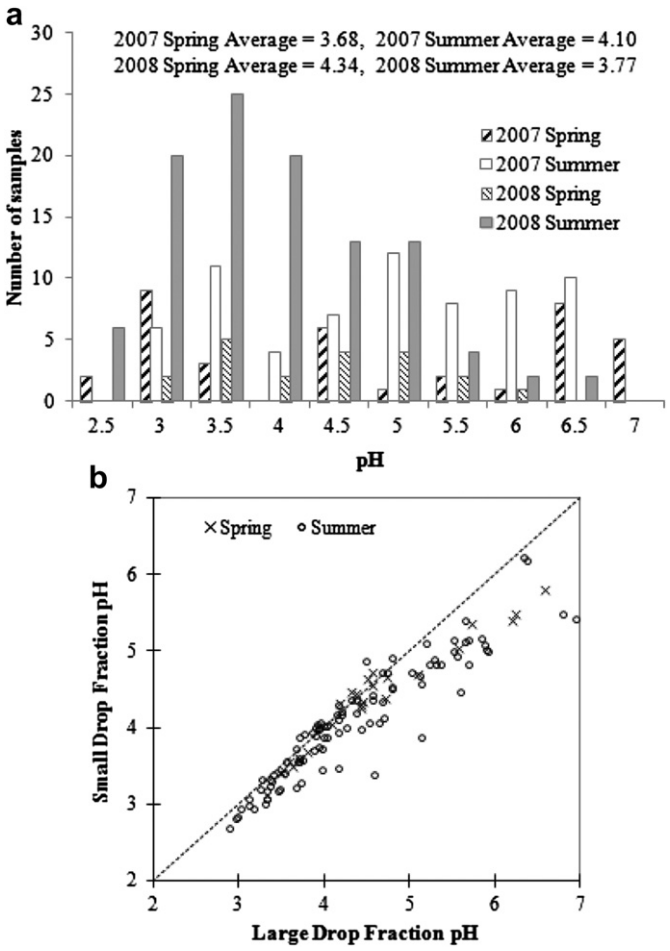

Fig. 3. (a) Frequency distributions of the pH values measured in bulk (CASCC) cloudwater samples during the four campaigns. (b) Comparison of the pH values measured in small ($4 < D < 16$ μm) and large ($D > 16$ μm) cloud drop size fractions simultaneously collected with the sf-CASCC during the spring and summer 2008 field campaigns. Drop size-fractionated samples were not collected in 2007.

campaigns. While only a small pH difference is observed between the small and large drop fractions during many sample periods, fairly large pH differences, of 0.5–1.0 pH units or greater, are observed in many other cases. The most common pattern is for large cloud drops to have a higher pH than small cloud drops, similar to the pattern first reported by Collett et al. (1994) for cloud and fog samples from a variety of environments. Differences in cloud composition as a function of drop size can arise from a variety of factors, including differences in the composition of cloud condensation nuclei (CCN) that nucleate small and large cloud drops, drop size-dependent condensational growth rates, and differences in the rate of uptake of soluble gases between small and large droplets (Bator and Collett, 1997; Moore et al., 2004a, 2004b; Ogren and Charlson, 1992). Understanding the distribution of pH values in a population of cloud drops can be important for accurately predicting rates of in-cloud sulfate production. Because the rates of some aqueous S(IV) oxidation pathways are nonlinear functions of the cloud drop H^+ concentration, the average H^+ concentration in a bulk cloudwater sample is not necessarily a good predictor of the average aqueous phase sulfate production rate (Collett et al., 1994; Gurciullo and Pandis, 1997; Hegg and Larson, 1990; Hoag et al., 1999; Reilly et al., 2001; Seidl, 1989).

As catalysts of the S(IV) autooxidation pathway, the aqueous concentrations of Fe(III) and Mn(II) are also important to examine.

Frequency distributions of bulk cloudwater Fe and Mn concentrations observed at Mt. Tai in the four sampling campaigns are shown in Fig. 4. The average bulk cloudwater Fe concentrations measured in spring and summer 2007 were 242 μg L^{-1} and 44.2 μg L^{-1}, respectively. Fe concentrations measured in spring and summer 2008 averaged 242 μg L^{-1} and 416 μg L^{-1}, respectively. For comparison, total Fe was below 400 μg L^{-1} in Los Angeles basin cloudwater samples (Pehkonen et al., 1992), averaged approximately 250 μg L^{-1} in clouds sampled at Great Dun Fell, U.K. (Sedlak et al., 1997), was below 500 μg L^{-1} in clouds collected at the puy de Dome station in France (Parazols et al., 2006) and ranged up to 886 μg L^{-1} in San Joaquin Valley, California fogs (Rao and Collett, 1998). The average Mn concentrations observed in spring and summer 2007 were 93.2 μg L^{-1} and 30.2 μg L^{-1}, respectively. Mn concentrations in spring and summer 2008 averaged 20.4 μg L^{-1} and 29.9 μg L^{-1}, respectively. Collett et al. (1999) reported Mn concentrations as high as 118 μg L^{-1} in San Joaquin Valley, California fogs. Comparisons of the small and large cloud drop size fraction concentrations of Fe and Mn are illustrated in Fig. 5, based on 2008 samples collected with the sf-CASCC. No consistent pattern of trace metal enrichment in either large or small cloud drops is observed, although considerable concentration differences are observed between the drop size fractions in many cases. Drop size-dependent concentrations of Fe and Mn have also previously been reported in radiation fogs and stratiform clouds from a variety of locations in the United States (Moore et al., 2004a, 2004b; Rao and Collett, 1998; Reilly et al., 2001). As in the case of the H^+ concentration, the non-linear dependence of the metal-catalyzed S(IV) autooxidation pathway on the metal concentrations can result in the average cloudwater metal concentration being a poor predictor of the average rate of S(IV) oxidation by this pathway (Rao and Collett, 1998), a topic that will be addressed below.

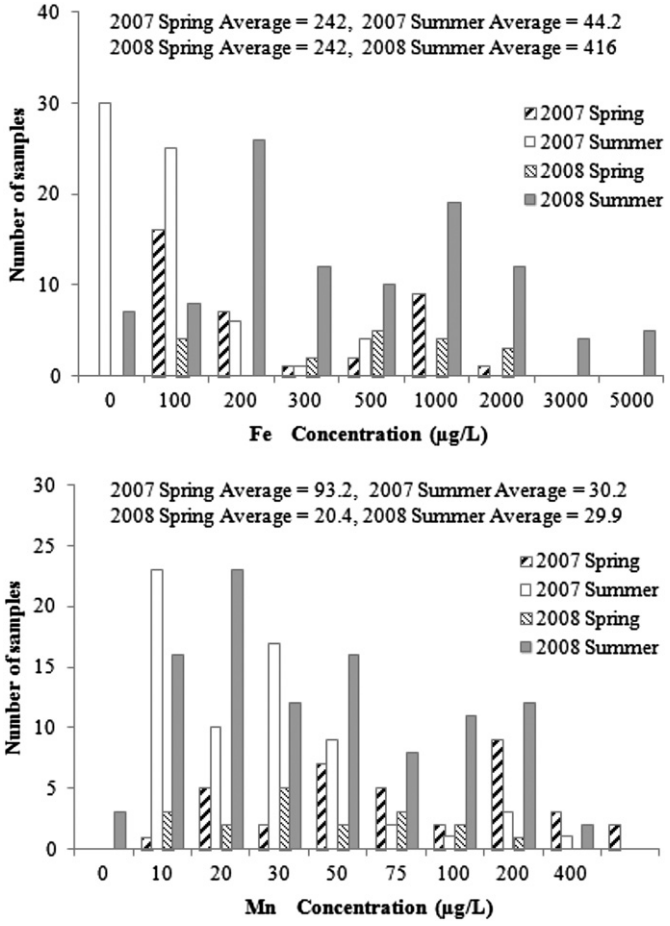

Fig. 4. Frequency distributions of Fe (top panel) and Mn (bottom panel) concentrations measured in bulk (CASCC) cloudwater samples collected at Mt. Tai in the four sampling campaigns.

Formaldehyde and other carbonyl compounds can also be important players in aqueous S(IV) chemistry in clouds. The complexation of formaldehyde with dissolved S(IV), can lead to formation of hydroxymethanesulfonate (HMS) (Boyce and Hoffmann, 1984; Munger et al., 1984, 1986; Olson and Hoffmann, 1989). HMS formation tends to be important mainly at pH values above 5–6 (Rao and Collett, 1995), because the formation rate increases quickly as pH rises. Formaldehyde concentrations measured in cloudwater collected at Mt. Tai were generally fairly modest, with average concentrations of 21.3 μM and 25.4 μM, in spring and summer 2007, and average concentrations of 4.7 μM and 9.5 μM in spring and summer 2008 (Fig. 6). Little difference was typically observed between HCHO concentrations measured in large and small cloud drop fractions collected with the sf-CASCC, consistent with expectations of equilibrium partitioning between gas and aqueous phase HCHO across the cloud drop size spectrum.

3.3. Sulfur oxidation rates

Utilizing the cloudwater and gas phase measurements described above, we can compute rates of aqueous phase S(IV) oxidation by H_2O_2, by O_3, and by O_2 with trace metal (Fe(III) and Mn(II)) catalysis. Literature rate expressions (Hoffmann, 1986; Hoffmann and Calvert, 1985; Ibusuki and Takeuchi, 1987; Seinfeld and Pandis, 2006) used for these calculations are listed in Table 1. Rate and equilibrium constants were adjusted using published thermodynamic data to represent the ambient temperature at the sampling site during each sample period. In completing the rate calculations, aqueous H_2O_2 and O_3 concentrations were determined assuming Henry's Law equilibrium with the measured gas phase concentrations during the period the cloud sample was collected. The measured aqueous cloudwater H_2O_2 concentration was not considered appropriate to use in these calculations because it can be rapidly consumed by reaction with S(IV) during the time (ranging from a few minutes up to 1–2 h) between cloud drop impaction on the collector strands and retrieval and chemical stabilization of the cloud sample. The H_2O_2 concentration was assumed to be 0.1 ppbv during periods in spring 2008 when valid gas phase H_2O_2 concentrations were not available. Concentrations of H_2SO_3, HSO_3^-, and SO_3^{2-} in solution were determined from measured gaseous SO_2 concentrations and measured cloudwater pH, assuming Henry's Law and acid base equilibria. The H^+ concentration was taken from the measured cloud sample pH. Metal catalyst concentrations were taken from measured cloud sample Fe and Mn concentrations. Following the approach of Rao and Collett (1995), the Mn was assumed to be completely present as catalytically active Mn(II) and 25% of the Fe was assumed to be present as catalytically active Fe(III).

Oxidation rates calculated for each bulk cloudwater sample for each of these three oxidation pathways are depicted in Fig. 7a. Among the three S(IV) oxidation pathways, oxidation by H_2O_2 was generally found to be the fastest pathway for pH values less than approximately 5. A doubling or halving of the 0.1 ppb H_2O_2 mixing ratio assumed for spring 2008 samples has little effect on this conclusion. The oxidation rate is linear in the H_2O_2 concentration while the reaction rates are plotted in Fig. 7a on a logarithmic axis. Further, less than 10% of the cloud samples were collected in spring 2008 when measured H_2O_2 mixing ratios were not available. The importance of O_3 as an oxidant increased strongly as pH values

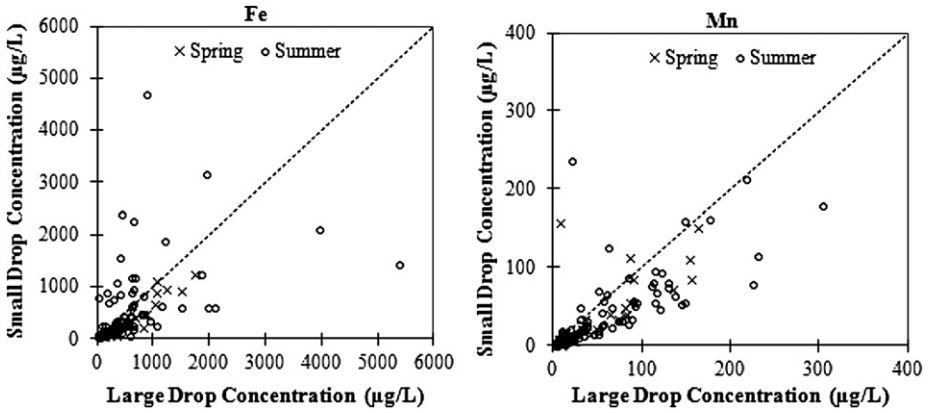

Fig. 5. Comparisons of the Fe (left panel) and Mn (right panel) concentrations measured in small ($4 < D < 16$ μm) and large ($D > 16$ μm) cloud drop size fractions simultaneously collected with the sf-CASCC during the spring and summer 2008 field campaigns. Drop size-fractionated samples were not collected in 2007.

climbed above 5–5.3. Variations in the rate of S(IV) oxidation by ozone show little overall dependence on the ozone concentration. This is because the influence of cloudwater pH is much stronger. At higher pH H_2SO_3–HSO_3^-–SO_3^{2-} partitioning shifts toward the deprotonated S(IV) forms; this increases the SO_2 oxidation rate because more SO_2 is drawn into solution and the S(IV) speciation shifts toward more reactive forms. These general tendencies are known behaviors of these oxidation pathways, although the pH where the transition occurs depends on local conditions, including the relative abundance of H_2O_2 and O_3.

Computed metal-catalyzed S(IV) autooxidation rates, also shown in Fig. 7a, are highly variable, reflecting high variability in cloudwater trace metal concentrations and the nonlinear dependence of the Ibusuki and Takeuchi (1987) rate expression on these concentrations. In general, the rate of this oxidation pathway is typically 2nd or 3rd fastest of the three computed oxidation pathways across the full observed pH range. There are some periods, however, where the metal-catalyzed pathway appears fast enough to make an important contribution to aqueous sulfate production.

Fig. 7b depicts the total S(IV) oxidation rate for each sample period, determined as the sum of the H_2O_2, O_3, and metal-catalyzed autooxidation rates. Here one clearly sees the relative lack of dependence on pH below pH ~5 (variations in H_2O_2 abundance are important here) and the rapid increase in aqueous sulfate production rates at higher pH values. The total oxidation rate patterns depicted in Fig. 7b are fairly similar for the 2007 and 2008 cloud samples, suggesting that these patterns are fairly robust under a variety of emission, cloud formation, and transport patterns. Note that the 2008 summer campaign period concluded before the start of the 2008 Beijing Olympics when more stringent regional emissions reductions came online. Grouping all 4 measurement campaigns together, we find that in 68% of the sample periods the fastest S(IV) oxidation pathway is the hydrogen peroxide pathway. The ozone pathway is fastest 20% of the time and the metal-catalyzed pathway is fastest 12% of the time.

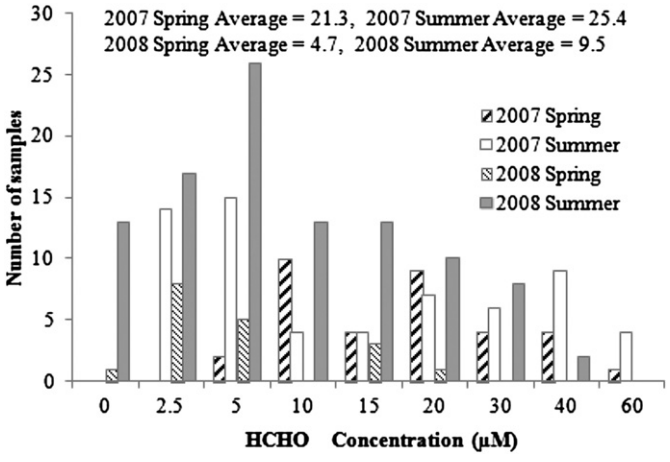

Fig. 6. Frequency distributions of HCHO concentrations measured in Mt. Tai bulk (CASCC) cloudwater samples.

Given the abundant SO_2 often found in the regional atmosphere, it is somewhat surprising to see that H_2O_2 remained present at sufficient concentrations to be the dominant oxidant so much of the time. In addition to the gas phase H_2O_2 observations used for the oxidation rate calculations, we can also examine the presence of H_2O_2 in the collected cloudwater. While there are many samples where H_2O_2 was low (or was depleted by reaction prior to sample retrieval and derivatization), there are also many samples, especially from the summertime, where tens to hundreds of μM of H_2O_2 remain in the cloudwater and little S(IV) remained (see Fig. 8). This residual peroxide indicates a substantial capacity during these periods for additional in-cloud sulfate production. Interestingly, several samples included in Fig. 8 contain both residual H_2O_2 and residual S(IV). This could reflect either the presence of S(IV) in a nonreactive form (e.g., complexed with HCHO as HMS) or continued aqueous photochemical production of H_2O_2 up until the point of sample collection and preservation.

Fig. 7a depicts rates of HMS formation due to reaction of dissolved S(IV) with HCHO. These rates were computed using the expression by Boyce and Hoffmann (1984). Aqueous S(IV) concentrations and speciation were determined as outlined above for the oxidation rate concentrations. HCHO concentrations were taken from the measured HCHO concentrations in the individual cloud samples. Because these HCHO values may include some HMS already present in the cloudwater (HCHO is preserved as HMS following sample collection), these rates should be considered an upper limit to the actual HMS formation rate in Mt. Tai clouds. While HMS formation does not appear important at low pH values, the calculations suggest that it may provide an additional, important sink for dissolved SO_2 when cloud pH climbs much above 4. Future cloud composition studies in the region should include direct measurement of HMS to determine whether its formation is as important as suggested by the rate calculations here. Measured S(IV) concentrations in Mt. Tai cloudwater, which would also include any HMS present at the time of cloud sample collection, place an upper limit on the amount of HMS production. S(IV)

Table 1
Rate expressions used for S(IV) oxidation and S(IV) reaction with HCHO.

Reaction rate (M s^{-1})	Characteristic time (s)	Reference
$-\frac{d[S(IV)]}{dt} = (k_0\alpha_0 + k_1\alpha_1 + k_2\alpha_2)[S(IV)][O_3]$	$\tau_{O_3} = 1/((k_0\alpha_0 + k_1\alpha_1 + k_2\alpha_2)[O_3])$	(Hoffmann and Calvert, 1985)
$-\frac{d[S(IV)]}{dt} = \frac{k[H^+][H_2O_2][S(IV)]\alpha_1}{1+K[H^+]}$	$\tau_{H_2O_2} = (1+K[H^+])/(k[H^+][H_2O_2]\alpha_1)$	(Seinfeld and Pandis, 2006)
$-\frac{d[S(IV)]}{dt} = k_s'[H^+]^{-0.74}[Fe(III)]\cdot[Mn(II)]\cdot[S(IV)]$	$\tau'_{O_2(Mn(II)/Fe(III))} = 1/(k_s'[H^+]^{-.74}[Fe(III)]\cdot[Mn(II)])$	(Ibusuki and Takeuchi, 1987)
$-\frac{d[S(IV)]}{dt} = k_s''[H^+]^{0.67}[Fe(III)]\cdot[Mn(II)]\cdot[S(IV)]$	$\tau''_{O_2(Mn(II)/Fe(III))} = 1/(k_s''[H^+]^{0.67}[Fe(III)]\cdot[Mn(II)])$ $6.5 \geq pH \geq 4.2$	(Ibusuki and Takeuchi, 1987)
$-\frac{d[S(IV)]}{dt} = k_4[S(IV)]\alpha_1[HCHO] + k_5[S(IV)]\alpha_2[HCHO]$	$\tau_{HCHO} = 1/([HCHO]\cdot(k_4\alpha_1 + k_5\alpha_2))$	(Boyce and Hoffmann, 1984)

α_0, α_1, and α_2 represent the fractions of total free S(IV) present as $SO_2\cdot H_2O$, HSO_3^- and SO_3^{2-}, respectively. $k_0 = 2.4\times10^4$ $M^{-1}s^{-1}$, $k_1 = 3.7\times10^5$ $M^{-1}s^{-1}$, $k_2 = 1.5\times10^9$ $M^{-1}s^{-1}$, $k = 7.45\times10^7$ $M^{-2}s^{-1}$, $K = 13$ M^{-1}, $k_4 = 7.9\times10^2$ $M^{-1}s^{-1}$, $k_5 = 2.48\times10^7$ $M^{-1}s^{-1}$ at 298 K; $k_s' = 3.72\times10^7$ $M^{-2}s^{-1}$ and $k_s'' = 2.51\times10^{13}$ $M^{-2}s^{-1}$ at 296.8 K.

exhibited a broad concentration range, although the average concentration in each of the four measurement campaigns was 40 μM or less, far below average sulfate concentrations.

Comparisons between S(IV) oxidation rates computed for small and large cloud drop size fractions collected in 2008 with the sf-CASCC are shown in Fig. 9 for the ozone and metal-catalyzed pathways. There is a tendency for oxidation rates to be higher in the large drops. This comes from the strong dependence of both pathways on cloud pH (faster oxidation at higher pH) and the tendency (see Fig. 3b) for the pH to be higher in the large cloud drop size fraction. In the case of the metal-catalyzed pathway, there is also an effect from any drop size-dependence in the Fe and Mn concentrations.

The (volume-weighted) average oxidation rate in a cloud, predicted from the oxidation rates in the large and small drop size fractions does not necessarily equal the oxidation rate predicted from the (volume-weighted) average cloud composition. While the averaging order does not matter for the hydrogen peroxide pathway, which exhibits no dependence on drop size, it can be important for the ozone and metal-catalyzed pathways. The nonlinear dependence of these two pathways on the H^+ concentration (and the metal catalyst concentrations in the latter case) can lead to substantially different results for the two methods. We can define an oxidation enhancement ratio, resulting from chemical heterogeneity among droplet composition in a cloud, as the ratio of the volume-weighted average oxidation rate divided by the oxidation rate calculated using the volume-weighted average composition. Fig. 10 shows the oxidation enhancement ratios for the three oxidation pathways, based on the sf-CASCC small and large drop composition and sample volume data. As indicated above, no enhancement occurs for the hydrogen peroxide pathway. The ozone pathway shows a maximum oxidation enhancement factor of 4.2, with enhancement factors for several sample periods

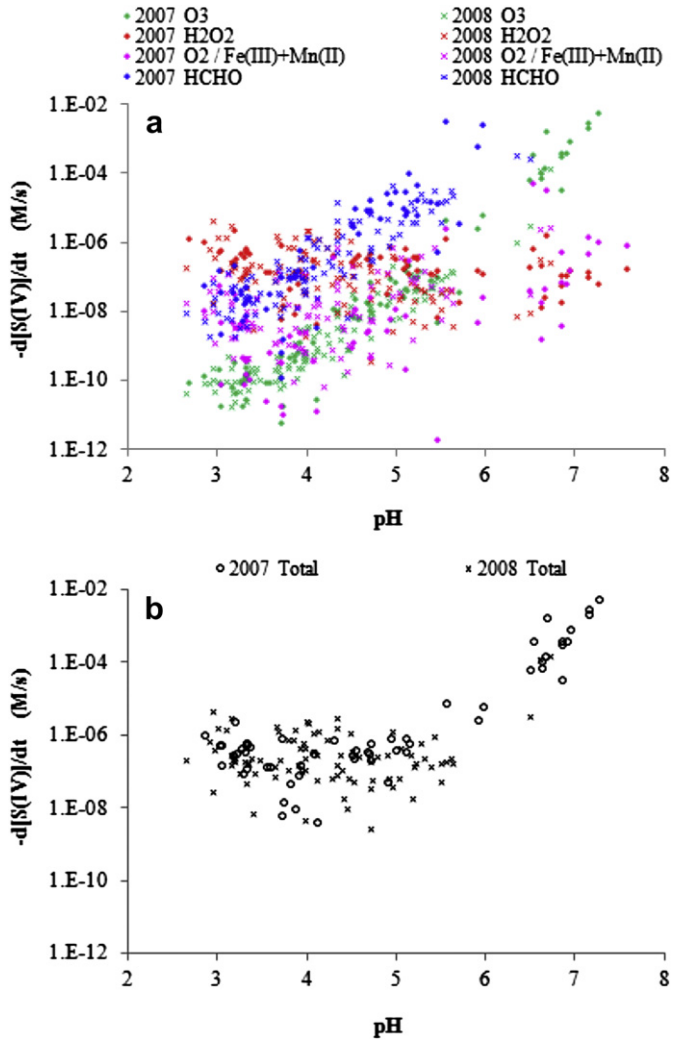

Fig. 7. S(IV) reaction rates determined for individual bulk cloudwater samples (panel (a)) according to the approach outlined in the text. Rates of reaction are included for S(IV) oxidation by O_3, by H_2O_2, and by O_2 (catalyzed by Fe and Mn) and for S(IV) reaction with HCHO to form HMS. Total S(IV) oxidation rates (panel (b)) determined for each sampling period.

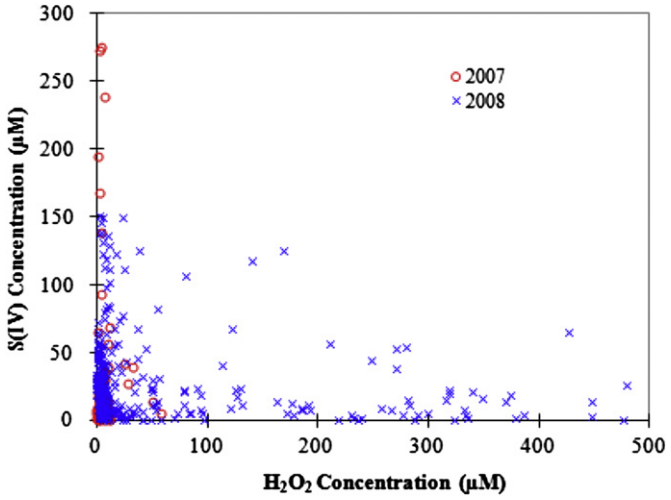

Fig. 8. Concentrations of aqueous H_2O_2 and S(IV) measured in Mt. Tai cloudwater collected in 2007 and 2008.

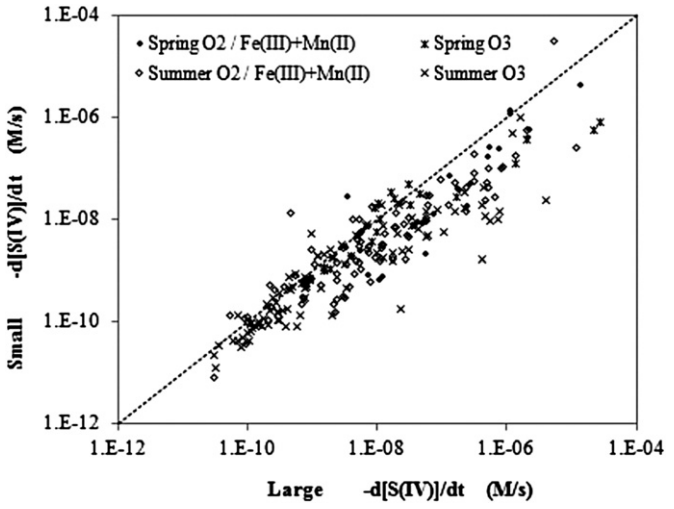

Fig. 9. Comparison of predicted S(IV) oxidation rates in small ($4 < D < 16$ μm) and large ($D > 16$ μm) cloud drop size fraction sample pairs collected in 2008 with the sf-CASCC. Results are shown for the ozone and metal-catalyzed autooxidation pathways.

falling in the range of 1.5–3. The median enhancement factor for the ozone pathway is 1.07 and 55% of values fall between 1.0 and 1.1. The enhancement factors for the metal-catalyzed pathway range from 0.2 to 2.4. Values less than 1.0 occur when metal catalyst concentrations are higher in the more acidic drop fraction. The median enhancement factor for the metal-catalyzed pathway is 1.08; 31% of values fall between 0.8 and 1.0 and 34% of values fall between 1.0 and 1.2. These results indicate the importance of considering chemical heterogeneity among the composition of droplets within Mt. Tai clouds to accurately portray rates of S(IV) oxidation by the ozone and metal-catalyzed pathways. The results here, which are based on only two independent cloud compositions, should be considered a lower bound on the true ozone and metal-catalyzed pathway oxidation enhancement present in the clouds, which likely contain a much wider variety of droplet compositions. Total S(IV) oxidation rates (the sums of all three oxidation pathways) in Mt. Tai clouds, however, are less sensitive to chemical heterogeneity among cloud drop composition since

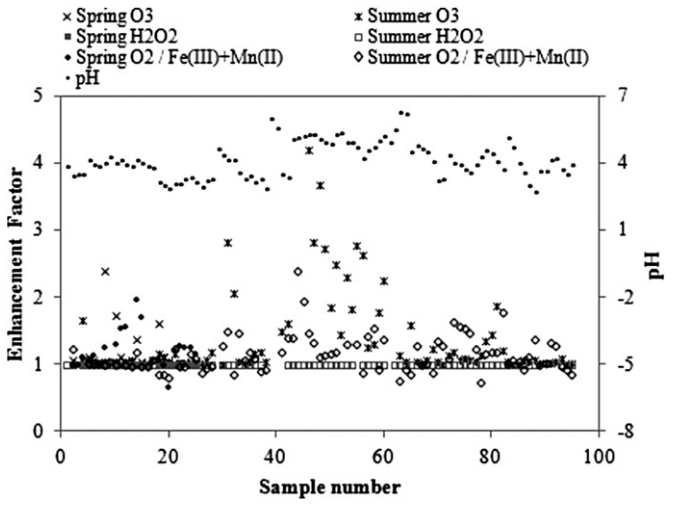

Fig. 10. Sulfur oxidation enhancement factors determined using the 2008 sf-CASCC dataset. The enhancement factor is defined as the volume-weighted average oxidation rate divided by the oxidation rate predicted from the volume-weighted average cloud composition. See text for details.

hydrogen peroxide was observed to be the dominant oxidant in most of the cloud periods measured.

4. Conclusions

Considering the large SO_2 emissions in China and the importance of aqueous phase oxidation processes for sulfate production, it is imperative to understand factors influencing regional cloud chemistry in order to predict accurately effects of increasing Chinese SO_2 emissions on sulfate production in that part of the world and its local, regional, and intercontinental effects. Sulfate production is critically important both to production of acid precipitation and to regional climate forcing. Four field campaigns conducted in 2007 and 2008 at Mt. Tai in eastern China provide direct insight into aqueous phase sulfur chemistry, the relative importance of different S(IV) oxidation pathways, and the ability of regional clouds to support aqueous sulfate production.

S(IV) oxidation showed relatively little pH dependence for cloud pH values below 5, where H_2O_2 was generally the dominant oxidant. The importance of O_3 as an oxidant increased strongly as pH values climbed above 5–5.3. Metal-catalyzed S(IV) autooxidation rates were highly variable. Overall, in 68% of the sample periods the fastest S(IV) oxidation pathway was the hydrogen peroxide pathway. The ozone pathway was fastest 20% of the time and the metal-catalyzed pathway was fastest 12% of the time. While high ambient SO_2 concentrations and results from previous numerical simulations suggested that sulfate production in regional clouds should be peroxide limited, this was clearly not always the case as indicated by these findings regarding the dominant oxidation pathway and by the observations of high concentrations of residual hydrogen peroxide, especially in summer cloudwater. Uncertainty remains about the importance of S(IV) complexation by formaldehyde, a mechanism that should be examined more closely in future studies.

These data provide a novel and robust dataset for evaluating numerical simulations of the fate of SO_2 emitted in China and their impacts on formation of local acid precipitation, on visibility and regional climate forcing, and on long-range transport of submicron sulfate aerosol particles. The importance of H_2O_2 as an aqueous phase oxidant is clear and, for the first time, the presence of residual H_2O_2 (and associated additional capacity for rapid aqueous phase sulfate production) in many summertime clouds has been demonstrated. In addition, measurements of the composition of clouds at Mt. Tai clearly reveal that China's air pollution has moved well beyond the point where sulfur dioxide and dust emissions are the only concerns. Abundant cloudwater ammonium, nitrate and organic matter clearly demonstrate the importance of other pollutant emissions in regional cloud chemistry.

Acknowledgments

This work was supported by the US National Science Foundation (ATM-0711102) and by the National Basic Research Program of China (973 Program) (2005CB422203). We are grateful to Mr. Tingli Sun, Wei Nie, and Rui Gao (Shandong University) for assistance in the field campaigns.

References

Anastasio, C., Faust, B.C., Allen, J.M., 1994. Aqueous phase photochemical formation of hydrogen peroxide in authentic cloud waters. J. Geophys. Res. Atmos. 99, 8231–8248.

Barth, M.C., Church, A.T., 1999. Regional and global distributions and lifetimes of sulfate aerosols from Mexico City and southeast China. J. Geophys. Res. Atmos. 104, 30231–30239.

Barth, M.C., Rasch, P.J., Kiehl, J.T., Benkovitz, C.M., Schwartz, S.E., 2000. Sulfur chemistry in the National Center for Atmospheric Research Community Climate Model: description, evaluation, features, and sensitivity to aqueous chemistry. J. Geophys. Res. Atmos. 105, 1387–1415.

Bator, A., Collett, J.L., 1997. Cloud chemistry varies with drop size. J. Geophys. Res. Atmos. 102, 28071–28078.

Boyce, S.D., Hoffmann, M.R., 1984. Kinetics and mechanism of the formation of hydroxymethanesulfonic acid at low pH. J. Phys. Chem. 88, 4740–4746.

China-MEP, 2010. 2009 Report on the State of the Environment in China. http://jcs.mep.gov.cn/hjzl/zkgb/2009hjzkgb/201006/t20100603_190429.htm.

Collett, J.L., Bator, A., Rao, X., Demoz, B.B., 1994. Acidity variations across the cloud drop size spectrum and their influence on rates of atmospheric sulfate production. Geophys. Res. Lett. 21, 2393–2396.

Collett, J.L., Hoag, K.J., Sherman, D.E., Bator, A., Richards, L.W., 1999. Spatial and temporal variations in San Joaquin Valley fog chemistry. Atmos. Environ. 33, 129–140.

Dasgupta, P.K., Decesare, K., Ullrey, J.C., 1980. Determination of atmospheric sulfur dioxide without tetrachloromercurate(II) and the mechanism of the Schiff reaction. Anal. Chem. 52, 1912–1922.

Demoz, B.B., Collett, J.L., Daube, B.C., 1996. On the Caltech Active Strand Cloudwater Collectors. Atmos. Res. 41, 47–62.

Dong, S., Dasgupta, P.K., 1987. Fast fluorometric flow injection analysis of formaldehyde in atmospheric water. Environ. Sci. Technol. 21, 581–588.

Faust, B.C., Anastasio, C., Allen, J.M., Arakaki, T., 1993. Aqueous-phase photochemical formation of peroxides in authentic cloud and fog waters. Science 260, 73–75.

Gao, J., Wang, T., Ding, A.J., Liu, C.B., 2005. Observational study of ozone and carbon monoxide at the summit of Mount Tai (1534 m a.s.l.) in central-eastern China. Atmos. Environ. 39, 4779–4791.

Gerber, H., 1991. Direct measurement of suspended particulate volume concentration and far-infrared extinction coefficient with a laser-diffraction instrument. Appl. Opt. 30, 4824–4831.

Guo, J., Wang, Y., Shen, X., Wang, Z., Lee, T., Wang, X., Li, P., Sun, M., Collett J.L., Jr., Wang, W., Wang, T., 2012. Characterization of cloud water chemistry at Mt. Tai, China: seasonal variation, anthropogenic impact, and cloud processing. Atmos. Environ 60, 467–476.

Gurciullo, C.S., Pandis, S.N., 1997. Effect of composition variations in cloud droplet populations on aqueous-phase chemistry. J. Geophys. Res. Atmos. 102, 9375–9385.

Hegg, D.A., Larson, T.V., 1990. The effects of microphysical parameterization on model predictions of sulfate production in clouds. Tellus 42B, 272–284.

Hoag, K.J., Collett, J.L., Pandis, S.N., 1999. The influence of drop size-dependent fog chemistry on aerosol processing by San Joaquin Valley fogs. Atmos. Environ. 33, 4817–4832.

Hoffmann, M.R., 1986. On the kinetics and mechanism of oxidation of aquated sulfur dioxide by ozone. Atmos. Environ. 20, 1145–1154.

Hoffmann, M.R., Calvert, J.G., 1985. Chemical Transformation Modules for Eulerian Acid Deposition Models. In: The Aqueous-Phase Chemistry, vol. II. National Center for Atmospheric Research, Boulder, CO.

Ibusuki, T., Takeuchi, K., 1987. Sulfur dioxide oxidation by oxygen catalyzed by mixtures of manganese(II) and iron(III) in aqueous solutions at environmental reaction conditions. Atmos. Environ. 21, 1555–1560.

Kanaya, Y., Komazaki, Y., Pochanart, P., Liu, Y., Akimoto, H., Gao, J., Wang, T., Wang, Z., 2008. Mass concentrations of black carbon measured by four instruments in the middle of Central East China in June 2006. Atmos. Chem. Phys. 8, 7637–7649.

Kim, Y.J., Woo, J.H., Ma, Y.I., Kim, S., Nam, J.S., Sung, H., Choi, K.C., Seo, J., Kim, J.S., Kang, C.H., Lee, G., Ro, C.U., Chang, D., Sunwoo, Y., 2009. Chemical characteristics of long-range transport aerosol at background sites in Korea. Atmos. Environ. 43, 5556–5566.

Krotkov, N.A., Carn, S.A., Krueger, A.J., Bhartia, P.K., Yang, K., 2006. Band Residual Difference algorithm for retrieval of SO_2 from the Aura Ozone Monitoring Instrument (OMI). IEEE Trans. Geosci. Remote Sens. 44, 1259–1266. http://dx.doi.org/10.1109/TGRS.2005.861932.

Larssen, T., Lydersen, E., Tang, D.G., He, Y., Gao, J.X., Liu, H.Y., Duan, L., Seip, H.M., Vogt, R.D., Mulder, J., Shao, M., Wang, Y.H., Shang, H., Zhang, X.S., Solberg, S., Aas, W., Okland, T., Eilertsen, O., Angell, V., Liu, Q.R., Zhao, D.W., Xiang, R.J., Xiao, J.S., Luo, J.H., 2006. Acid rain in China. Environ. Sci. Technol. 40, 418–425.

Lazrus, A.L., Kok, G.L., Gitlin, S.N., Lind, J.A., McLaren, S.E., 1985. Automated fluorometric method for hydrogen peroxide in atmospheric precipitation. Anal. Chem. 57, 917–922.

Lazrus, A.L., Kok, G.L., Lind, J.A., Gitlin, S.N., Heikes, B.G., Shetter, R.E., 1986. Automated fluorometric method for hydrogen peroxide in air. Anal. Chem. 58, 594–597.

Lelieveld, J., Heintzenberg, J., 1992. Sulfate cooling effect on climate through in-cloud oxidation of anthropogenic SO_2. Science 258, 117–120.

Li, J., Pochanart, P., Wang, Z.F., Liu, Y., Yamaji, K., Takigawa, M., Kanaya, Y., Akimoto, H., 2008. Impact of chemical production and transport on summertime diurnal ozone behavior at a mountainous site in North China Plain. Sola 4, 121–124.

Mao, T., Wang, Y.S., Xu, H.H., Jiang, J., Wu, F.K., Xu, X.B., 2009. A study of the atmospheric VOCs of Mount Tai in June 2006. Atmos. Environ. 43, 2503–2508.

Moore, K.F., Sherman, D.E., Reilly, J.E., Collett, J.L., 2004a. Drop size-dependent chemical composition in clouds and fogs. Part I. Observations. Atmos. Environ. 38, 1389–1402.

Moore, K.F., Sherman, D.E., Reilly, J.E., Hannigan, M.P., Lee, T., Collett, J.L., 2004b. Drop size-dependent chemical composition of clouds and fogs. Part II: relevance to interpreting the aerosol/trace gas/fog system. Atmos. Environ. 38, 1403–1415.

Munger, J.W., Jacob, D.J., Hoffmann, M.R., 1984. The occurrence of bisulfite-aldehyde addition-products in fogwater and cloudwater. J. Atmos. Chem. 1, 335–350.

Munger, J.W., Tiller, C., Hoffmann, M.R., 1986. Identification of hydroxymethanesulfonate in fog water. Science 231, 247–249.

Ogren, J.A., Charlson, R.J., 1992. Implications for models and measurements of chemical inhomogeneities among cloud droplets. Tellus 44B, 208–225.

Olson, T.M., Hoffmann, M.R., 1989. Hydroxyalkylsulfonate formation: its role as a S(IV) reservoir in atmospheric water droplets. Atmos. Environ. 23, 985–997.

Parazols, M., Marinoni, A., Amato, P., Abida, O., Laj, P., Mailhot, G., 2006. Speciation and role of iron in cloud droplets at the puy de Dome station. J. Atmos. Chem. 54, 267–281.

Park, R.J., Jacob, D.J., Field, B.D., Yantosca, R.M., Chin, M., 2004. Natural and transboundary pollution influences on sulfate–nitrate–ammonium aerosols in the United States: implications for policy. J. Geophys. Res. Atmos. 109, 20.

Pehkonen, S.O., Erel, Y., Hoffmann, M.R., 1992. Simultaneous spectrophotometric measurement of Fe(II) and Fe(III) in atmospheric water. Environ. Sci. Technol. 26, 1731–1736.

Rao, X., Collett, J.L., 1995. Behavior of S(IV) and formaldehyde in a chemically heterogeneous cloud. Environ. Sci. Technol. 29, 1023–1031.

Rao, X., Collett, J.L., 1998. The drop size-dependence of iron and manganese concentrations in clouds and fogs: implications for sulfate production. J. Atmos. Chem. 30, 273–289.

Rattigan, O.V., Reilly, J., Judd, C.D., Moore, K.F., Das, M., Sherman, D.E., Dutkiewicz, V.A., Collett, J.L., Husain, L., 2001. Sulfur dioxide oxidation in clouds at Whiteface Mountain as a function of drop size. J. Geophys. Res. Atmos. 106, 17347–17358.

Reilly, J.E., Rattigan, O.V., Moore, K.F., Judd, C., Sherman, D.E., Dutkiewicz, V.A., Kreidenweis, S.M., Husain, L., Collett, J.L., 2001. Drop size-dependent S(IV) oxidation in chemically heterogeneous radiation fogs. Atmos. Environ. 35, 5717–5728.

Ren, Y., Ding, A.J., Wang, T., Shen, X.H., Guo, J., Zhang, J.M., Wang, Y., Xu, P.J., Wang, X.F., Gao, J., Collett, J.L., 2009. Measurement of gas-phase total peroxides at the summit of Mount Tai in China. Atmos. Environ. 43, 1702–1711.

Sedlak, D.L., Hoigne, J., David, M.M., Colvile, R.N., Seyffer, E., Acker, K., Wiepercht, W., Lind, J.A., Fuzzi, S., 1997. The cloudwater chemistry of iron and copper at Great Dun Fell, UK. Atmos. Environ. 31, 2515–2526.

Seidl, W., 1989. Ionic concentrations and initial S(IV)-oxidation rates in droplets during the condensational stage of cloud. Tellus 41B, 32–50.

Seinfeld, J.H., Pandis, S.N., 2006. Atmospheric Chemistry and Physics: from Air Pollution to Climate Change. John Wiley & Sons, Inc., New York.

Shen, X., 2011. Aqueous Phase Sulfate Production in Clouds at Mt. Tai in Eastern China, Ph.D. dissertation, Colorado State University, 3454634, Available Online from UMI/ProQuest at: http://gradworks.umi.com/34/54/3454634.html, 193 pp.

Wai, K.M., Tanner, P.A., Tam, C.W.F., 2005. 2-Year study of chemical composition of bulk deposition in a south China coastal city: comparison with east Asian cities. Environ. Sci. Technol. 39, 6542–6547.

Wang, G.H., Kawamura, K., Umemoto, N., Xie, M.J., Hu, S.Y., Wang, Z.F., 2009. Water-soluble organic compounds in $PM_{2.5}$ and size-segregated aerosols over Mount Tai in North China Plain. J. Geophys. Res. Atmos. 114, 10.

Wang, T., Cheung, T.F., Li, Y.S., Yu, X.M., Blake, D.R., 2002. Emission characteristics of CO, NO_x, SO_2 and indications of biomass burning observed at a rural site in eastern China. J. Geophys. Res. Atmos. 107, 10.

Wang, T., Cheung, V.T.F., Anson, M., Li, Y.S., 2001. Ozone and related gaseous pollutants in the boundary layer of eastern China: overview of the recent measurements at a rural site. Geophys. Res. Lett. 28, 2373–2376.

Wang, T., Ding, A.J., Gao, J., Wu, W.S., 2006a. Strong ozone production in urban plumes from Beijing, China. Geophys. Res. Lett. 33, 5.

Wang, T., Poon, C.N., Kwok, Y.H., Li, Y.S., 2003. Characterizing the temporal variability and emission patterns of pollution plumes in the Pearl River Delta of China. Atmos. Environ. 37, 3539–3550.

Wang, Y., Guo, J., Wang, T., Ding, A.J., Gao, J.A., Zhou, Y., Collett, J.L., Wang, W.X., 2011. Influence of regional pollution and sandstorms on the chemical composition of cloud/fog at the summit of Mt. Taishan in northern China. Atmos. Res. 99, 434–442.

Wang, Y., Wai, K.M., Gao, J., Liu, X.H., Wang, T., Wang, W.X., 2008. The impacts of anthropogenic emissions on the precipitation chemistry at an elevated site in north-eastern China. Atmos. Environ. 42, 2959–2970.

Wang, Z.F., Li, J., Wang, X.Q., Pochanart, P., Akimoto, H., 2006b. Modeling of regional high ozone episode observed at two mountain sites (Mt. Tai and Huang) in east China. J. Atmos. Chem. 55, 253–272.

Yamaji, K., Li, J., Uno, I., Kanaya, Y., Irie, H., Takigawa, M., Komazaki, Y., Pochanart, P., Liu, Y., Tanimoto, H., Ohara, T., Yan, X., Wang, Z., Akimoto, H., 2010. Impact of open crop residual burning on air quality over central eastern China during the Mount Tai Experiment 2006 (MTX2006). Atmos. Chem. Phys. 10, 7353–7368.

Zuo, Y.G., Deng, Y.W., 1999. Evidence for the production of hydrogen peroxide in rainwater by lightning during thunderstorms. Geochim. Cosmochim. Acta 63, 3451–3455.